JOURNAL OF GEOPHYSICAL RESEARCH, VOL. 104, NO. D21, PAGES 26,097-26,105, NOVEMBER 20, 1999

Comparison of tropospheric NO_3 radical measurements by differential optical absorption spectroscopy and matrix isolation electron spin resonance

A. Geyer and B. Alicke
Institut für Umweltphysik, Universität Heidelberg, Heidelberg, Germany

D. Mihelcic
Institut für Atmosphärische Chemie, Forschungszentrum Jülich, Jülich, Germany

J. Stutz and U. Platt
Institut für Umweltphysik, Universität Heidelberg, Heidelberg, Germany

Abstract. Despite the importance of NO_3 in the nighttime atmosphere only two techniques, Differential Optical Absorption Spectroscopy (DOAS) and Matrix Isolation Electron Spin Resonance (MIESR) have been applied to its detection in ambient air to date. Here we report the results of the first intercomparisons of these techniques in the atmosphere carried out at rural sites in Germany, at Deuselbach in 1983 and near Berlin in 1998. The simultaneously measured NO_3 mixing ratios, which were in the range from 9 to 20 ppt and at one measurement near 100 ppt, were in good agreement within the error limits. A regression analysis yields a linear relationship between the DOAS and MIESR data with a correlation coefficient of $R = 0.99$ and a slope of 0.83 ± 0.03 (1σ error) at a negligible intercept of 0.33 ± 0.73 ppt (1σ error). The deviation from unity is within the total systematic error of both measurement techniques. This result shows the reliability of the two techniques over the past 15 years.

1. Introduction

Free radicals play an important role as catalysts in the complex atmospheric photochemical system. Besides the photochemically produced hydroxyl radical (OH) and ozone (O_3), the nitrate radical (NO_3) is the driving force for the degradation of many volatile organic compounds (VOC), in particular, olefinic species. In addition, nitrate radicals initiate the formation of peroxy radicals (HO_2 and RO_2) and hydroxyl radicals (OH) at night [*Platt et al.*, 1990; *Mihelcic et al.*, 1993].

Because of their high reactivity, the measurement of nitrate radicals is a challenge for any analytical technique employed. A number of different analytical techniques based on optical absorption in the visible region [*Hautefeuille and Chappuis*, 1881], infrared absorption [*Cramarossa and Johnston*, 1965], laser-induced fluorescence (LIF) [*Ishiwata et al.*, 1983; *Nelson et al.*, 1983], mass spectrometry [*Benter and Schindler*, 1988], or electron spin resonance (ESR) [Chantry et al., 1962] were used in the laboratory. However, since the first detection of nitrate radicals in the troposphere by *Platt et al.* [1980] and *Noxon et al.* [1980], only two techniques have been successfully applied to atmospheric NO_3 measurement: the long path Differential Optical Absorption Spectroscopy (DOAS) [*Platt et al.*, 1979] and the Matrix Isolation Electron Spin Resonance (MIESR) [*Mihelcic et al.*, 1982]. While the long path DOAS technique is based on the absorption of UV and visible light by nitrate radicals and a number of other trace gases (e.g., HONO, NO_2, SO_2, O_3, HCHO, aromatic hydrocarbons, halogen oxides) integrated along a light path in the atmosphere of several kilometers, MIESR attends to the para-magnetic properties of NO_3 and other free radicals (RO_2, HO_2, NO_2). Both methods have been shown to be powerful techniques for tropospheric NO_3 measurements at various locations at comparable sensitivity. The advantages of DOAS are its good time resolution of few minutes and the contact-free determination, thus eliminating the possibility of reactions on the surface of a sampler. In comparison, the advantage of MIESR is its capability to perform in situ measurements. With respect to the importance of nitrogen oxides for our understanding of atmospheric chemistry, it is very important to compare these different measurement techniques to assess the accuracy and reliability of the tropospheric NO_3 determination. While it is not possible to compare NO_3 measurements with a calibrated standard gas, both techniques need to prove their correctness by simultaneous measurements in the atmosphere.

In this paper, we present recent results of an intercomparison of tropospheric NO_3 measurements by DOAS and MIESR performed at a rural site (Pabstthum) in Brandenburg, Germany, within the framework of the "Berliner Ozonexperiment" (BERLIOZ). The DOAS measurements were carried out by a long path DOAS system developed at the Institute for Environmental Physics, University of Heidelberg. The MIESR system was constructed at the Research Center Jülich.

Paper number 1999JD900421.
0148-0227/99/1999JD900421$09.00

In addition, earlier simultaneous measurements of NO_3 in Deuselbach, Germany, were reevaluated using the improved numerical analytical procedure described in detail by *Mihelcic et al.* [1990] to eliminate the interference of the ESR spectra of NO_3 and RO_2 which led to a large uncertainty of the NO_3 mixing ratios determined by MIESR in the original evaluation made in 1983.

2. Experimental Section

2.1. Description of the DOAS Measurement Technique for NO_3

The fundamental setup of a DOAS system monitors the integrated absorption of the nitrate radicals along a light path in the atmosphere. The concentration of NO_3 can be derived by applying the Beer-Lambert law:

$$c = \frac{\ln {}^{I_0(\lambda)}/_{I(\lambda)}}{\sigma(\lambda)L} \quad (1)$$

where c denotes the concentration of NO_3 (molecules/cm^3), $\sigma(\lambda)$ the absorption cross section of NO_3 at the wavelength λ, and L the length of the light path. $I(\lambda)$ and $I_o(\lambda)$ are the light intensities with and without absorption by NO_3 and other trace gases. Introducing the optical density $D = \ln (I_o(\lambda)/I(\lambda))$, (1) can be written as:

$$c = \frac{D(\lambda)}{\sigma(\lambda)L} \quad (2)$$

In the atmosphere, it is not possible to determine $I_o(\lambda)$ due to unknown extinction by broadband Rayleigh and Mie scattering. The basic idea of DOAS is to separate the trace gas absorption cross section into two parts: one that varies slowly with wavelength and a quickly varying differential cross section. As the spectral characteristic of the atmospheric aerosol extinction processes vary slowly with the wavelength, DOAS analyses only the narrow absorption structures. This separation of the cross section can be performed by numerical filters as described elsewhere [*Platt*, 1994]. The concentrations of the absorbing trace gases can then be derived by comparing reference spectra of the relevant species, which were treated with the same filter, to the spectrum measured in the atmosphere.

2.1.1. Setup of the long path DOAS systems. The long path DOAS system used in Pabstthum was a modern version of the original setup developed by *Platt et al.* [1979]. The light source was a 500 W Xe high-pressure arc lamp (Hanovia 959C1980). The spectrograph was an ACTON Spectra Pro 500 with a focal length of 500 mm (f/6.9, entrance slit 0.15 mm, dispersion 3.12 nm/mm (or 0.078 nm/pixel), spectral resolution 0.6 nm, thermostated at 30 ± 0.2°C) with a plane diffraction grating. For recording the spectra, a 1024 pixel photodiode array detector (Hoffmann Meßtechnik, photodiode array: Hamamatsu S5931-1024N, cooled to –30 ± 0.2°C) was mounted in the focal plane of the spectrograph. For a more detailed description of the system see *Stutz and Platt* [1997].

During the Deuselbach intensives in 1983, a 240 W tungsten-iodine lamp served as light source. The spectrograph was a SPEX 1870 (focal length 500 mm, grating 600 grooves/mm). A thin metal disk etched with exit slits (100 μm wide) rotating in the focal plane of the spectrograph was used to scan the spectrum. The light passing through the slits was monitored by a photomultiplier with S20 cathode (EMI 9558 QB). The spectral resolution was 0.3 – 0.4 nm. A more detailed description of the DOAS system in Deuselbach is given by *Platt et al.* [1981].

2.1.2. DOAS data evaluation. Discussion of the DOAS data evaluation is given here for the reference spectra and the evaluation procedure.

2.1.2.1. Reference spectra: The absorption cross section $\sigma(\lambda)$ of the nitrate radical shows strong features in the red spectral region with prominent bands at wavelengths of 662 nm and 623 nm, respectively (see Figure 1 (trace E)). In this work the temperature independent absorption cross section $\sigma(662\ \text{nm}) = (2.1 \pm 0.2)10^{-17}$ cm^2 recommended by *Wayne et al.* [1991] was used as a DOAS reference spectrum for the NO_3 evaluation in Pabstthum (1998) and Deuselbach (1983, recalibration). This cross section was derived by averaging the data of four recent studies *of Ravishankara and Mauldin* [1986], *Sander* [1986], *Cantrell et al.* [1987], and *Canosa-Mas et al.* [1987]. A comparison of the different studies of the NO_3 cross section is given in section 4.

Besides NO_3, water vapor, oxygen, and NO_2 have differential absorption structures in the investigated spectral region (600 - 680 nm). In addition, a broad xenon emission line (corresponding to an optical density D = - 1.5%) from the high-pressure arc lamp strongly interferes with the water absorption structure at 649 nm. Under tropospheric conditions, water vapor usually shows the strongest absorption features in

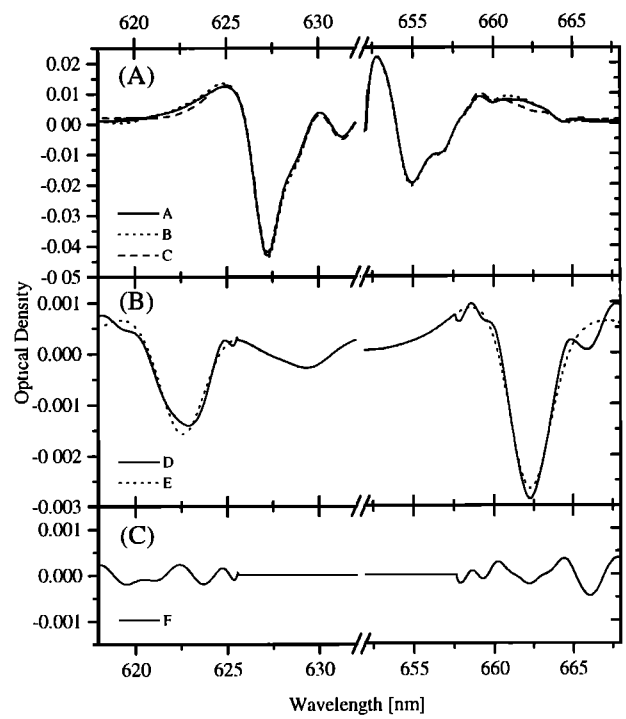

Figure 1. NO_3 analysis by long path DOAS in Pabstthum (1998). (A) Two atmospheric daytime spectra (trace B: August 4, 1702 UT, SZA=78.9°; trace C: August 5, 0419 UT, SZA=75.6°) were used to subtract H_2O absorption features from the nighttime spectrum (trace A: August 4, 2150 UT). (B) The residual spectrum (trace D) after fitting of B and C to A clearly shows the absorption structure of NO_3 (trace E) with a concentration of 9.8 ± 1.1 ppt. (C) The residual structure after simultaneous fitting of B, C, and E to A.

the red spectral region. At the low resolution of our spectrograph (0.6 nm) a combination of very strong absorption lines appear as weak absorption bands in the spectra (see Figure 2, trace B - D). During BERLIOZ, water vapor mixing ratios of 1% to 1.8% were observed, resulting in optical densities near 647 nm of the order of 0.2 - 0.3 at our resolution. At these high water vapor column densities (defined as $S := [H_2O] \times L$, where L is the length of the light path) of the order of 4×10^{23} cm^{-2}, the individual H_2O lines have optical densities in excess of unity. Because of the convolution with the spectral line shape of our instrument function the optical density is no longer linearly dependent on S. Considering the variation of the water vapor column amount during BERLIOZ, a model study was carried out to investigate the effects of this nonlinear dependence of H_2O absorption bands on the results of our NO_3 evaluation. Different optical densities of water vapor were simulated by applying Lambert-Beer's law to the high-resolution water absorption cross section [*Rothmann*, 1992] and then smoothing the calculated spectrum to simulate our instrumental resolution. This simulation demonstrates that the column amount dependent absorption structure of H_2O can be interpolated by simultaneously fitting two water reference spectra, which enclose the optical density of the atmospheric spectrum (see Figure 2). The resulting residual structures caused by an incorrect elimination of the water vapor absorption are a factor of 3 below the detection limit of NO_3. Changes of the water vapor absorption structure due to variations of temperature and pressure [*Aliwell and Jones*, 1996] could be significantly reduced and therefore neglected by the selection of the water vapor reference spectra and the parameters of the numerical filters and the fitting area: the NO_3 data evaluation was restricted to the wavelength intervals 618 – 626 nm and 657 – 668 nm (see Figure 1). Because of this restriction of the fitting area, the absorption features of oxygen, NO_2, and the broad Xe-emission band at 649 nm can be neglected in the NO_3 data evaluation. Since NO_3 only exists at detectable concentrations during the night, daytime spectra (at solar zenith angles < 80°) can serve as reference spectra for water absorption. In Pabstthum the best results were achieved using two daytime spectra recorded close to the studied night. At Deuselbach, only one daytime reference spectrum was used, resulting in water absorption residual structures, which were almost 4 times larger compared to the evaluation of the Pabstthum spectra.

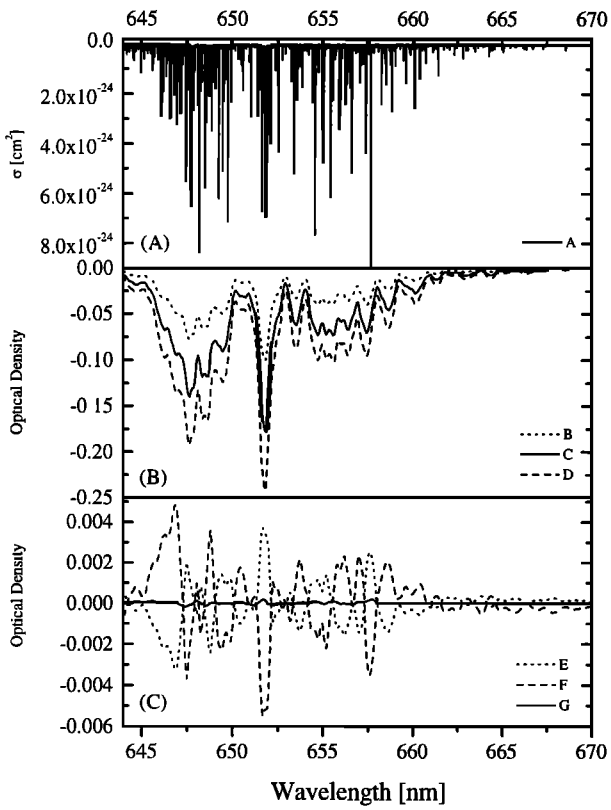

Figure 2. Simulation of the column amount dependence of the water vapor absorption. (A) Calculated absorption lines at the high resolution of 0.005 nm (trace A). (B) Calculated optical densities of water vapor absorption at 296 K and 1013 hPa using the low resolution of our spectrograph (0.6 nm) and water vapor mixing ratios of 0.01 (trace B), 0.014 (trace C), and 0.018 (trace D). (C) The residual structures after fitting B to C (trace E), D to C (trace F), and B and D (simultaneously) to C (trace G), corresponding to optical densities of 1%, 0.7%, and 0.035%, respectively.

2.1.2.2. Evaluation procedure: In a first step, electronic offset and background light were corrected by subtraction from the measured atmospheric spectra. The logarithm of the resulting spectrum was then numerically band-pass filtered by first subtracting a smoothed (2500-times "triangular" smoothing) copy of the spectrum and then low-pass filtering (100-times "triangular" smoothing) the result. Thus high-frequency (shot-) noise as well as broadband extinction structures due to atmospheric Rayleigh and Mie scattering and possible broadband molecular absorbers were greatly reduced. The parameters of high-pass filter and smoothing were derived by minimizing the statistical error of the evaluated NO_3 concentrations. The two daytime water vapor reference spectra and the NO_3 reference spectrum were subjected to the same filtering technique and were fitted to the measured spectrum simultaneously using a least squares routine described by *Stutz and Platt* [1996]. While no spectral "shift" and "squeeze" was allowed for the NO_3 reference spectra, a simultaneous shift and squeeze was permitted for the two daytime reference spectra.

Figure 1 provides an example of the NO_3 evaluation of the DOAS data from Pabstthum. It shows the two atmospheric daytime spectra used to eliminate water vapor absorption features from the nighttime spectrum. The residual structure after removing H_2O absorption from the spectrum clearly indicates the spectral signature of NO_3 with a concentration of 9.8 ± 1.1 ppt.

The error of the least squares fitting procedure underestimates the "true" statistical error [*Stutz and Platt*, 1996] and must be corrected by multiplication with a factor, which was calculated by subjecting modeled atmospheric spectra to the NO_3 evaluation procedure to be about 6 (1σ error). During BERLIOZ, a mean true statistical error (all errors in this paper refer to the 1σ error) of the NO_3 concentration of 1.1 ppt was observed with variations due to changes in water vapor concentration and lamp parameters. The uncertainty of the NO_3 absorption cross section can be assumed as ±10% (see above) [*Wayne et al.*, 1991]. The length of the atmospheric light path was determined (within an uncertainty of <1%) as the difference in the apparent position of two simultaneously operated Global Positioning System (GPS) receivers at either end of the (folded) light path. The systematic error of the DOAS

spectrometer was determined by *Stutz* [1996] as <3%. The total systematic error of the NO_3 concentrations determined by DOAS is therefore <14%.

2.2. Description of the MIESR Measurement Technique for NO_3

2.2.1. Background. Quantitative determinations of nitrate radicals in the troposphere using the Matrix Isolation Electron Spin Resonance (MIESR) technique were first reported by *Mihelcic et al.* [1985] with subsequent developments and applications described by *Mihelcic et al.* [1990, 1993] and *Volz et al.* [1988].

Briefly, the samples were collected by pumping ambient air into an evacuated cryosampler through a 0.16 mm diameter critical nozzle that restricted the flow rate to 15 sL/h (standard liters per hour). The radicals were trapped on gold-plated copper cold fingers in polycrystalline D_2O-ice matrices at a temperature of 77 K. The use of D_2O instead of H_2O as the matrix reduces the line widths and therefore yields a better spectral resolution of NO_2, NO_3, HO_2 and RO_2. The accompanying increase in the peak to peak amplitude results in a greater sensitivity of NO_2, NO_3, HO_2, and $CH_3C(O)O_2$ in D_2O by a factor of 1.4, 1.9, 1.9, and 1.6, respectively [*Mihelcic et al.*, 1990]. In Pabstthum (1998) the cryosampler was mounted on a pneumatic mast using a free rotating inlet nozzle with a wind vane to ensure that the nozzle pointed into the wind to avoid contamination by both the sampler and the reservoir of liquid N_2. In Deuselbach (1983) the MIESR samples were collected by an earlier version of the cryosampler described previously [*Mihelcic et al.*, 1985]. During both campaigns, the collection efficiency exceeded 95%.

2.2.2. Data acquisition and evaluation. Following sampling, the samples were analyzed with an ESR spectrometer in our laboratory. The samples collected in Deuselbach (1983) were analyzed with a Varian-E Line ESR-spectrometer equipped with a V4535 cavity. The samples collected in Pabstthum (1998) were analyzed with a Bruker ESP 300E spectrometer with a ER 4109 WZS widebore cavity.

On the Bruker ESP 300E ESR spectrometer, normally a scan width of 200 G (2 min sweep time, 0.25 s RC-time constant) is used. The modulation amplitude is (0.5 - 2) G, depending on the width of the spectral features to be resolved (a greater modulation amplitude results in a better signal-to-noise ratio). About 100 individual scans of each spectrum are recorded and digitally averaged in order to improve the signal-to-noise ratio. The digital resolution (1024 channels for 200 G sweep width) is 0.2 G and thus at least twice as large as that given by the modulation amplitude.

2.2.2.1. Reference spectra: Reference spectra for the analysis of atmospheric samples of a variety of different radicals were recorded in the laboratory. The radicals were prepared in a flow system at 1050 hPa and 298 K in pure D_2O matrices. The preparation procedures for NO_2, HO_2, and $CH_3C(O)O_2$ were reported by *Mihelcic et al.* [1985]. NO_3 radicals were generated by reaction of fluorine atoms with HNO_3 in argon. Alkylperoxy radicals were produced by the reaction of chlorine atoms with the respective alkanes. Fluorine and chlorine atoms were formed in a corona discharge

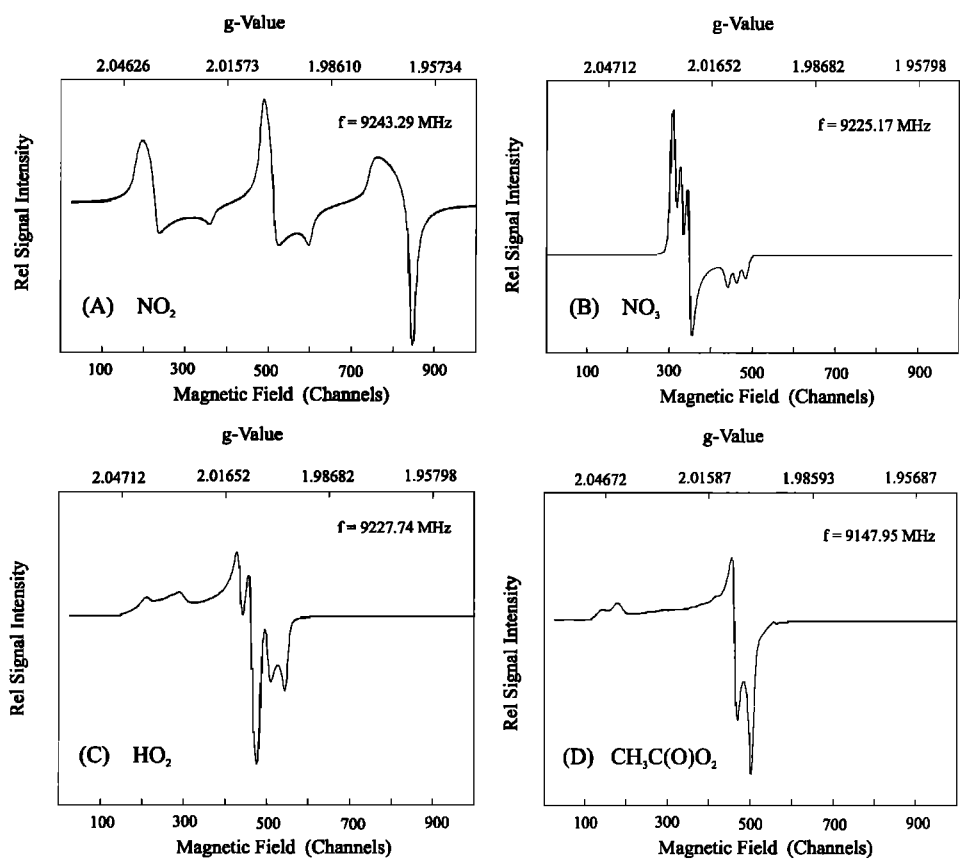

Figure 3. ESR spectra of NO_2 (trace A), NO_3 (trace B), HO_2 (trace C) and $CH_3C(O)O_2$ radicals (trace D) trapped in D_2O matrices. All spectra were measured at 77 K, with a 2 G modulation amplitude, 200 G scan range (except for NO_3, scan range 100 G).

through mixture of 20 ppm F_2 and 0.5% Cl_2, respectively, in Ar, similar to the procedure described for hydrogen atoms [*Mihelcic et al.*, 1985]. Figure 3 shows ESR spectra of NO_2, NO_3, HO_2, and $CH_3C(O)O_2$ radicals at a temperature of 77 K. The experimental conditions were similar for all samples frozen in the D_2O matrices (77 K, 0.5 g of matrix material, radical/matrix ratio < 10^{-7}).

The NO_2 spectrum shows the well-known triplet due to interaction of the free electron with the nuclear spin of the ^{14}N atom. The HO_2 spectrum exhibits a characteristic hyperfine splitting as a result of the interaction of the free electron with the nuclear spin of the proton. The spectrum of $CH_3C(O)O_2$ is typical for peroxy radicals with a carbonyl group, without any interaction with protons. As in the case of NO_2, the spectrum of NO_3 shows a triplet splitting due to the interaction of the free electron with the nuclear spin of the ^{14}N atom.

2.2.2.2. Numerical analysis: Figure 4 provides an example of an ESR spectrum recorded on August 4 in Pabstthum (1998). It shows the relative signal intensity, i.e., the first derivative of the ESR absorption spectrum, as a function of the magnetic field. The uppermost spectrum (trace A) is that of the original air sample, which, as is evident by comparison with the NO_2 reference spectrum of trace B, is dominated by 4.3 ppb NO_2. Subtraction of the NO_2 yields the residual spectrum shown in trace C. Comparison with the reference spectra in traces D (NO_3) and E (the sum of RO_2 radicals) clearly indicates that the residual spectral signature in the ambient air sample comprises NO_3 and RO_2 with concentrations of 12.8 and 10 ppt, respectively, retrieved from the fit. Comparison of trace B and E in Figure 4 and corresponding reference spectra frozen in a pure D_2O matrix (Figure 3) shows that the spectra in real atmospheric samples are broader than the reference spectra. The broadening effect is more visible for the NO_3 spectrum (trace D, Figure 4), where the triplet structure of the reference spectrum is no longer visible. The broadening is due to the presence of 10 – 20% H_2O in the matrix, depending on absolute humidity during sample collection. Therefore different amounts of H_2O in the matrices of different samples yield ESR spectra with slightly variable line widths. A numerical procedure for the analysis of the composite ESR spectra obtained from atmospheric samples was developed and described by *Mihelcic et al.* [1990].

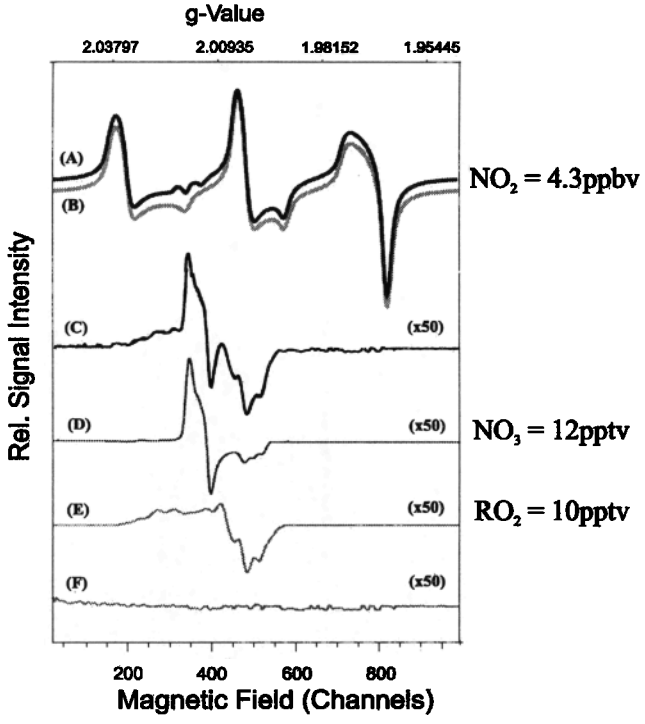

Figure 4. Relative signal intensity, or first derivative of the ESR absorption spectrum, as a function of the magnetic field. The uppermost spectrum (trace A) is that of the original air sample (August 4, 2200-2230 UT), which, as is evident by comparison with the NO_2 reference spectrum of trace B, is dominated by 4.3 ppb NO_2. Subtraction of the NO_2 yields the residual spectrum shown in trace C. Comparison with the reference spectra in traces D (NO_3) and E (the sum of RO_2) clearly indicates that the residual spectral signature in the ambient air sample comprises NO_3 and RO_2 with concentrations of 12 and 10 ppt, respectively, retrieved from the fit. Trace F shows the residual spectrum after subtraction of the NO_3 and RO_2 contribution.

Subtraction of the dominant NO_2 signal was performed by matching a reference NO_2 spectrum with respect to amplitude, spectral position, and line width to the sample spectrum. The fitting procedures were performed with the virtually noise-free reference spectrum.

As already demonstrated by *Mihelcic et al.* [1985], the NO_2 line at the highest magnetic field, that is, at $g = 1.965$ (channels $700 \leq k \leq 1000$ in Figure 4), is free of interferences by ESR lines of NO_3 and RO_2 radicals. Therefore, only this line (henceforth referred to as the third line) was used to match a NO_2 reference spectrum (Figure 4, trace B) to the composite spectrum of atmospheric samples. The main part of the fitting procedure for removal of the NO_2 structure was a least squares fit that changes amplitude, line width, and spectral position of the reference NO_2 spectrum. The NO_2 reference spectrum for the whole range of 1000 channels was then produced by using the parameters evaluated by the fit procedure in the range of the third NO_2 line. A precise determination of the residual spectrum was possible only after NO_2 had been removed from the atmospheric sample spectrum.

The residual spectrum only contains information from radicals other than NO_2, i.e., by RO_2 and NO_3. The contribution from specific radicals was determined by simultaneously fitting up to six different spectra of peroxy radicals and NO_3. The accuracy of this fit depends on the number of parameters that have to be optimized. In order to reduce this number and, more important, to avoid systematic errors regarding slight shifts in the spectral position of the RO_2 spectra from different atmospheric samples, we used NO_2 as an internal reference for the position in the magnetic field. In order to do so, the RO_2 and NO_3 reference spectra shown in Figure 4 were recorded from samples that contained, at the same time, small amounts of NO_2 (≈10%). These reference spectra were then matched to a given atmospheric sample spectrum by fitting the third NO_2 line to the optimized NO_2 reference spectrum. Besides the spectral position, the required information on the line width could also be obtained from the NO_2 spectrum. It was found that, within the resolution of our spectrometer, the lines of all radicals investigated are broadened in the same fashion. Therefore, only the amplitude scale factors for the different RO_2 and NO_3 spectra must be optimized (by the least squares fit) after NO_2 has been removed from the reference spectra.

The precision of the fit for HO_2, $CH_3C(O)O_2$, and ΣRO_2 is, over the whole range of concentrations, better than 3 ppt. The

precision of the fit for NO_3 radicals is < 2 ppt, due to its narrower ESR line width. The systematic uncertainty of the MIESR measurements of NO_3 was determined from absolute calibration as ±5%.

3. Results of the Intercomparisons

3.1. Comparison of the NO_3 Measurements at Pabstthum in 1998

The NO_3 measurements during BERLIOZ were performed at the edge of a 7.5 x 4.5 km² flat meadow in the vicinity of the small village of Pabstthum (12°56'25''E, 52°51'15''N, altitude 50 m above sea level). This rural site has little traffic so that local anthropogenic emissions can be neglected during the night. The metropolis of Berlin is situated to the SE (145°) at a distance of 50 km (center) and 35 km (suburbs), respectively. The city of Neuruppin is located to the NW (12 km). A highway passes 14 km to the south of the site. The light path of the DOAS system pointed in an easterly direction from a height of 1.5 m at the site to the reflector at a distance of 6.3 km and mounted 36 m above the ground. The total absorption light path was 12.6 km. The MIESR sampler was situated at the site 15 m above the ground. Measurements of other trace gases, meteorological parameters, and aerosols were performed (8 – 15) m above the ground.

Both NO_3 instruments operated in the night from August 4 to 5, 1998. The DOAS instrument started NO_3 measurements at 1740 UT just before sunset. Because of increasing haze, the DOAS measurements were stopped at 0220 UT. The mean time resolution of the DOAS data was 3 min resulting in 133 NO_3 data points for this night. MIESR measurements started at 2030, 2115, 2200, 2245, 2330, and 0021 UT. The sampling time was 30 min for each measurement. Figure 5 shows the time series of the DOAS and MIESR measurements for that night. After sunset, NO_3 mixing ratios quickly climbed to 10 ppt and remained at this level (range 7 – 12 ppt) until 2230 UT. During this period, three MIESR measurements were performed, which show good agreement within the statistical errors. At 2230 UT, NO_3 mixing ratios decreased, probably due to ground haze. Since NO_3 is rapidly depleted both directly and indirectly (via N_2O_5, which is in thermal equilibrium with NO_3) on aerosol surfaces [*Heikes and Thomson*, 1983; *Heintz et al.*, 1996], it is difficult to compare the NO_3 data of the two systems in the presence of ground haze: supposing a height of the ground haze of 18 m, the MIESR system would have been taken samples only from this haze layer, where NO_3 was strongly depleted. As the DOAS light beam ran from 1.5 m up to 36 m in height, only a part of the absorbing path would have been influenced by haze. Thus the NO_3 mixing ratios measured by DOAS should have been significantly higher than the MIESR data, as was actually the case (Figure 5).

3.2. Comparison of the NO_3 Measurements at Deuselbach in 1983

In addition to Pabstthum (1998), NO_3 had also been determined by parallel DOAS and MIESR measurements in Deu-

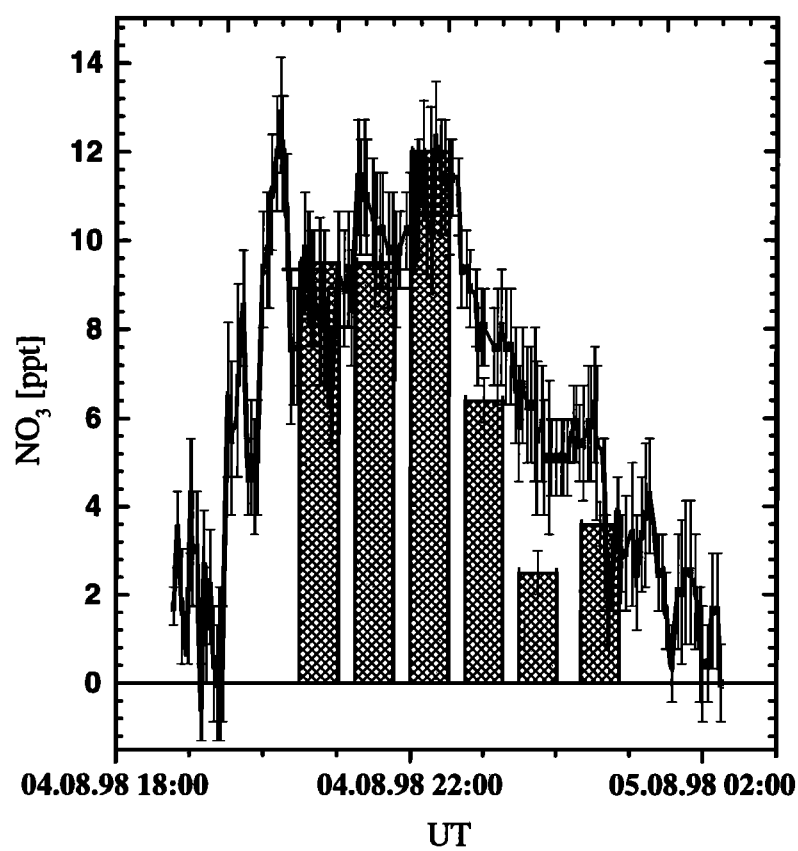

Figure 5. NO_3 mixing ratios measured by DOAS (line) and MIESR (bars) at Pabstthum, Germany, during the field campaign BERLIOZ (1998). The error bars refer to the statistical 1σ error. The mean time resolution of the DOAS data was 3 min. Sample time of the MIESR system was 30 min.

selbach, Germany, in May/June 1983. The village of Deuselbach (49°46'N, 7°3'E, 480 m above sea level) is situated in a rural area with negligible local anthropogenic emission sources during the night. The nearest cities are located 20 km (Idaroberstein) and 30 km (Trier) to the SE and W, respectively. During these measurements, the MIESR sampler was placed 5 m above the ground. The DOAS absorption path of 4.8 km ran from 1 to 150 m above the ground. Altogether, five measurements with NO_3 levels from 15 to ≈100 ppt were performed simultaneously over 3 days in May/June 1983 (May 16/17, May 19/20, and June 3/4) [*Platt et al.*, 1985]. In 1983, evaluation of the MIESR spectra was carried out with the help of a software package that did not allowed for correction of either the variable line width nor the simultaneous fitting of different spectra. In this work, the spectra were reevaluated using the improved numerical analytical procedure described in detail by *Mihelcic et al.* [1990], thereby significantly reducing the statistical errors of the NO_3 mixing ratios. The reason for the reevaluation was to eliminate interference of the ESR spectra of NO_3 and RO_2 leading to a large uncertainty of the NO_3 mixing ratios determined by MIESR in 1983. The concentrations determined by DOAS were recalculated with the absorption cross section suggested by *Wayne et al.* [1991]. Figure 6 shows the NO_3 mixing ratios measured by DOAS and MIESR for the three nights. Comparison of the NO_3 measurements again shows good agreement in the variation and the absolute values of the nighttime concentration profiles, with slightly higher values measured by MIESR.

3.3. Regression Analysis

The DOAS data were interpolated to the sampling time of the ESR measurements in order to compare the mixing ratios at appropriate times. A regression analysis, including weighting of the statistical errors of the measurement data of both techniques, of the interpolated data pairs of Deuselbach and Pabstthum was then carried out, yielding a slope of 0.83 ± 0.05 (DOAS versus MIESR) and an intercept of 0.33 ± 0.73 ppt with a correlation coefficient of $R = 0.99$ (see Figure 7). The intercept is not significant in view of the statistical errors of both techniques. To derive a correct regression, which is not influenced by different air mass sampling (e.g., due to ground haze), the last three data pairs of the Pabstthum intercomparison were excluded from the analysis. Since no intercomparison data exist from 20 to ~100 ppt, the regression is dominated by the one high data pair at about 100 ppt. Therefore Figure 7 also shows the regression analysis for the low concentration data only. The slope of this regression (0.68 ± 0.04, DOAS versus MIESR) is even lower, and the intercept is 2.96 ± 0.75 ppt with a correlation coefficient of $R = 0.99$. However, this analysis is dominated by the three low values from Pabstthum, where the measurements by

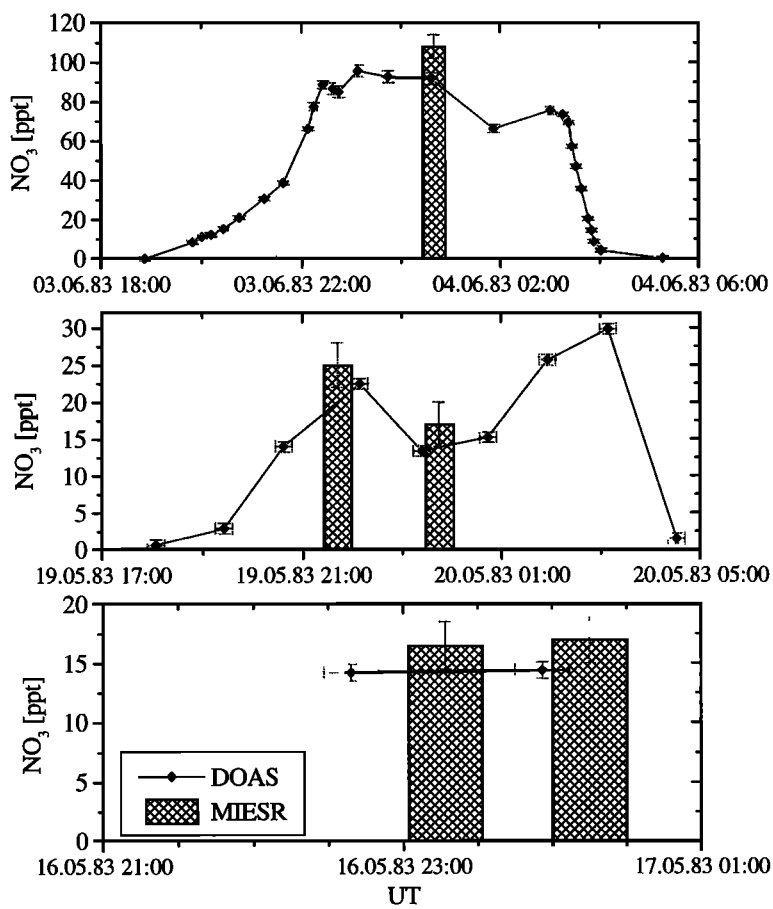

Figure 6. NO_3 mixing ratios measured by DOAS (line) and MIESR (bars) at Deuselbach, Germany, in May/June 1983. The MIESR data were revised according to the evaluation algorithm presented in this paper. The DOAS data were recalibrated to an absorption cross section of 2.1×10^{-17} cm^2. The error bars refer to the statistical 1σ error. Sample time of the MIESR system was 30 min.

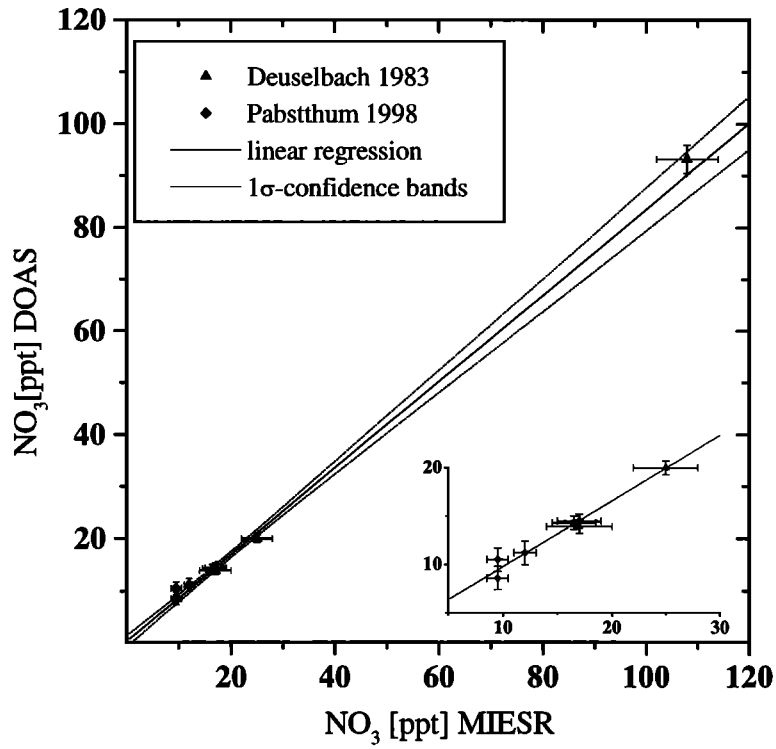

Figure 7. Intercomparison of the NO_3 mixing ratios simultaneously measured by DOAS and MIESR in Pabstthum (August 1998) and Deuselbach (May/June 1983). A linear regression analysis shows a good correlation of the two measurement techniques with a correlation coefficient $R = 0.99$.

MIESR are slightly higher than those by DOAS but, nevertheless, in agreement within the statistical uncertainty of both techniques.

4. Discussion and Conclusion

Two different techniques, DOAS and MIESR, were used to determine the concentration of tropospheric NO_3 during one night of the BERLIOZ field campaign in August 1998 near Berlin (Pabstthum). In addition, simultaneous measurements of DOAS and MIESR in Deuselbach (May/June 1983) were re-evaluated and recalibrated. To our knowledge, these two sets of measurements represent the only simultaneous determination of nitrate radicals in the atmosphere by different techniques.

Overall, 11 pairs of NO_3 concentrations were recorded simultaneously. Since both techniques did not analyze the same air volume, only eight data pairs under favorable meteorological conditions were used for intercomparison. The NO_3 mixing ratios, which were in the range from 9 to 20 ppt and at one measurement near 100 ppt, were in good agreement within the statistical errors of both techniques.

However, the linear regression yields slopes significantly lower than unity. This could be attributed to the analysis of air volumes at different heights by both systems, particularly during the Deuselbach intensives, when the DOAS system integrated the NO_3 concentration from 1 to 150 m above the ground, while the MIESR system sampled near the ground (5 m). Recent measurements and modeling studies [*Aliwell and Jones*, 1998; *Fish et al.*, 1999] show that there are times when, over this altitude range, there are gradients in the NO_3 concentration. However, Deuselbach is a rural site with no significant release of pollution in the measurement region. The measurements could have been influenced by different local biogenic sources of volatile organic compounds like monoterpenes, which can rapidly deplete nitrate radicals, leading to both a vertical and a horizontal variation of the NO_3 concentration. However, the result of sampling of different air masses should result in a variable effect for the intercomparison. Therefore the high correlation coefficient of $R = 0.99$ and the deviation of the slope from unity point rather to a systematic error. The deviation from unity of $17 \pm 5\%$ can be explained in view of the total systematic error of both systems of 19%, which is dominated by the uncertainty of the NO_3 absorption cross section of 10%. Deviation from unity would point to a cross section, which should be smaller than the value recommended by *Wayne et al.* [1991]. Various studies of the wavelength and temperature dependence of the NO_3 cross section have been performed in past years. While most of the studies report similar relative shapes of the spectrum there are discrepancies concerning the absolute value of $\sigma(\lambda)$ The value of the cross section at 298 K and 662 nm published by different authors varies from 1.21×10^{-17} cm^2 [*Mitchell et al.*, 1980] to 2.49×10^{-17} cm^2 [*Magnotta and Johnston*, 1980]. The most recent publication on the NO_3 cross section yielded $(2.23 \pm 0.22)10^{-17}$ cm^2 [*Yokelson et al.*, 1994]. Also the temperature dependence of the NO_3 absorption cross section is not clear. While *Sander* [1986], *Ravishankara and Mauldin* [1986], and *Yokelson et al.* [1994] determined an increase toward lower temperatures, *Cantrell et al.* [1987] did not find a temperature effect. As the temperature was in the range of 281 – 288 K for all nights involved in this intercomparison,

the use of the cross section published by *Yokelson et al.* [1994] of $\sigma(T) = (4.56 - 0.00788T)10^{-17}$ cm^2 (σ(281 K) = 2.35×10^{-17} cm^2, σ(288 K) = 2.29×10^{-17} cm^2) instead of *Wayne et al.'s* [1991] recommendation would result in lower DOAS values of the NO_3 concentration and thus lead to an even higher deviation of the slope from unity in the regression analysis. The difference of the cross section during the intercomparison (T = 281 – 288 K) therefore can account for a maximum 2% systematic deviation; thus temperature effects of the NO_3 cross section cannot explain the deviation from unity.

Future determinations of the NO_3 absorption cross section are therefore desirable.

Acknowledgment. Part of this project was supported by the BMBF in the framework of TFS (LT3, LT2) and KBF 52.

References

Aliwell, S. R., and R. L. Jones, Measurement of atmospheric NO_3, 1, Improved removal of water vapour absorption features in the analysis for NO_3, *Geophys. Res. Lett.*, *23*(19), 2585 – 2588, 1996.

Aliwell, S. R., and R. L. Jones, Measurement of tropospheric NO_3 at midlatitude, *J. Geophys. Res.*, *103*, 5719 – 5727, 1998.

Benter, T., and R. N. Schindler, Absolute rate coefficients for the reaction of NO_3 radicals with simple dienes, *Chem. Phys. Lett.*, *145*, 67-70, 1988.

Canosa-Mas, C. E., M. Fowles, P. J. Houghton, and R. P. Wayne, Absolute absorption cross section measurements on NO_3, *J. Chem. Soc. Faraday II*, *83*, 1465-1474, 1987.

Cantrell, C. A., J. A. Davidson, R. E. Shetter, B. A. Anderson, and J. G. Calvert, The temperature invariance of the NO_3 absorption cross-section in the 662 nm region, *J. Phys. Chem.*, *91*, 5858-5863, 1987.

Chantry G. W., A. Horsfield, J. R. Morton, and D. H. Whiffen, The structure, electron resonance and optical spectra of trapped CO_3 and NO_3, *Mol. Phys.*, *5*, 589-599, 1962.

Cramarossa, F., and H. S. Johnston, Infrared absorption by symmetrical NO_3 radicals in the gas phase, *J. Chem. Phys.*, *43*, 727-731, 1965.

Fish, D. J., D. E. Shallcross, and R. L. Jones, The vertical distribution of NO_3 in the atmospheric boundary layer, *Atmos. Environ.*, *33*, 687 – 691, 1999.

Hautefeuille, P., and J. Chappuis, De la recherche des composés gazeaux et de l'etude de quelques-unes de leurs propriétés à l'aide du spectroscope, *C. R. Acad. Sci. Paris*, *92*, 80-83, 1881.

Heikes, B. G., and A.M. Thomson, Effects of heterogeneous processes on NO_3, HONO, and HNO_3 chemistry in the troposphere, *J. Geophys. Res.*, *88*, 10,883-10,895, 1983.

Heintz F., H. Flentje, R. Dubois, and U. Platt, Long-term observation of nitrate radicals at the Tor Station, Kap Arkona (Rügen), *J. Geophys. Res.*, *101*, 22,891-22,910, 1996.

Ishiwata, T., I. Fujiwara, Y. Naruge, K. Obi, and I. Tanaka, Study of NO_3 laser induced fluorescence, *J. Phys. Chem.*, *87*, 1349-1352, 1983.

Magnotta, F., and H. S. Johnston, Photodissociation quantum yields for the NO_3 free radical, *Geophys. Res. Lett.*, *7*, 769-772, 1980.

Mihelcic, D., M. Helten, H. Fark, P. Müsgen, H. W. Pätz, M. Trainer, D. Kemp, and D. H. Ehhalt, Tropospheric airborne measurements of NO_2 and RO_2 using the technique of matrix isolation and electron spin resonance, paper presented at *the 2nd Symposium on Composition of the Nonurban Troposphere*, published by American Meteorological Society, Williamsburg, Va., 1982.

Mihelcic, D., P. Müsgen, and D. H. Ehhalt, An improved method of measuring tropospheric NO_2 and RO_2 by matrix isolation and electron spin resonance, *J. Atmos. Chem.*, *3*, 341-361, 1985.

Mihelcic, D., A. Volz-Thomas, H. W. Pätz, D. Kley, and M. Mihelcic, Numerical analysis of ESR spectra from atmospheric samples, *J. Atmos. Chem.*, *11*, 271-297, 1990.

Mihelcic, D., D. Klemp, P. Müsgen, H. W. Pätz, and A. Volz-Thomas, Simultaneous measurements of peroxy and nitrate radicals at Schauinsland, *J. Atmos. Chem.*, *16*, 313-335, 1993.

Mitchell, D. N., R. P. Wayne, P.J. Allan, R. P. Harrison, and R. J. Twin, Kinetics and photochemistry of NO_3, 1. Absolute cross-section, *J. Chem. Soc. Faraday II*, *76*, 785-793, 1980.

Nelson, H. H., L. Pasternack, and J. R. McDonald, Laser-induced excitation and emission spectra of NO_3, *J. Phys. Chem.*, *87*, 1286-1288, 1983.

Noxon, J. F., R. B. Norton, and E. Marovich, NO_3 in the troposphere, *Geophys. Res. Lett.*, *7*, 125-128, 1980.

Platt, U., Differential Optical Absorption Spectroscopy (DOAS), in *Monitoring by Spectroscopic Techniques*, edited by M. W. Sigrist, John Wiley, New York, 1994.

Platt, U., D. Perner, and H. W. Pätz, Simultaneous measurement of atmospheric CH_2O, O_3 and NO_2 by differential optical absorption, *J. Geophys. Res.*, *84*, 6329-6335, 1979.

Platt, U., D. Perner, G. W. Harris, A. M. Winer, and J. M. Pitts, Detection of NO_3 in the polluted troposphere by differential optical absorption, *Geophys. Res. Lett.*, *7*, 89-92, 1980.

Platt, U., D. Perner, H. Schroeder, G. Kessler, and A. Toenissen, The diurnal variation of NO_3, *J. Geophys. Res.*, *86*, 11,965-11,970, 1981.

Platt, U., D. Perner, and W. Junkermann, The atmospheric lifetime of nitrate radicals (NO_3), in *Proceedings COST 611 Symposium*, workgroups 4 and 5 on Pollutant cycles and transport: modelling and field experiments, edited by De Leeuw F. A., and N. D. van Egmond, 82-88, Bilthoven, Netherlands, 1985.

Platt, U., G. Le Bras, G. Poulet, J. P. Burrows, and G. K. Moortgat, Peroxy radicals from night-time reaction of NO_3 with organic compounds, *Nature*, *348*, 147-149, 1990.

Ravishankara, A. R., and R. L. Mauldin III., Temperature dependence of the NO_3 cross section in the 662 nm region, *J. Geophys. Res.*, *91*, 8709-8712, 1986.

Rothmann, L., HITRAN spectroscopic data, *J. Quant. Spectrosc. Radiat. Transfer*, *48*, 5 and 6, 1992.

Sander, S. P., Temperature dependence of the NO_3 absorption spectrum, *J. Phys. Chem.*, *90*, 4135-4142, 1986.

Stutz, J., Messung der Konzentration troposphärischer Spurenstoffe mittels Differentieller Optischer Absorptionsspektroskopie: Eine neue Generation von Geräten und Algorithmen. Ph.D. thesis, Inst. für Umweltphysik, Univ. Heidelberg, 1996.

Stutz, J., and U. Platt, Numerical analysis and error estimation of differential optical absorption measurements with least-squares methods, *Appl. Opt.*, *35*(30), 6041-6053, 1996.

Stutz, J., and U. Platt, Improving long path differential optical absorption spectroscopy with a quartz-fibre mode mixer, *Appl. Opt.*, *36*(6), 1105-1115, 1997.

Volz, A., D. Mihelcic, P. Müsgen, H. W. Pätz, G. Pilwat, H. Geiss, and D. Kley, Ozone production in the Black Forest: Direct measurements of RO_2, NO_x and other relevant parameters, in *Tropospheric Ozone - Regional and Global Scale Interactions*, edited by I.S.A. Isaksen, 293 pp., D. Reidel, Vorevell, Mass., 1988.

Wayne, R. P., et al., The nitrate radical: Physics, chemistry, and the atmosphere, *Atmos. Environ.*, *25A*, 1-203, 1991.

Yokelson, R. J., J. B. Burkholder, R. W. Fox, R. K. Talukdar, and A. R. Ravishankara, Temperature dependence of the NO_3 absorption, *J. Phys. Chem.*, *98*, 13,144-13,150, 1994.

B. Alicke, A. Geyer (corresponding author), U. Platt and J. Stutz, Institut für Umweltphysik, Universität Heidelberg, Im Neuenheimer Feld 229, 69120 Heidelberg, Germany. (andreas.geyer@iup.uni-heidelberg.de; ulrich.platt@iup.uni-heidelberg.de)

D. Mihelcic, Institut für Atmosphärische Chemie, Forschungszentrum Jülich, 52425 Jülich, Germany. (d.mihelcic@fz-juelich.de)

(Received April 9, 1999; revised June 7, 1999;
accepted June 9, 1999.)